Journal of Structural Geology 31 (2009) 817–830

Contents lists available at ScienceDirect

Journal of Structural Geology

journal homepage: www.elsevier.com/locate/jsg

Modelling of segment structures: Boudins, bone-boudins, mullions and related single- and multiphase deformation features

Xavier Maeder*, Cees W. Passchier, Daniel Koehn

Institut für Geowissenschaften, Johannes Gutenberg University, 55099 Mainz, Germany

ARTICLE INFO

Article history:
Received 10 July 2008
Received in revised form 19 May 2009
Accepted 25 May 2009
Available online 6 June 2009

Keywords:
Finite element modelling
Segment structure
Boudin
Tension gash
Flanking fold
General shear deformation

ABSTRACT

Finite element modelling has been used to simulate the development of segment structures, deformed layer segments separated by veins, such as boudins, mullions, and bone-boudins. A parameter sensitivity analysis is used to compare the influence of the nature of the flow, the relative viscosities of veins in necks and the host rock, and the initial geometry of the layer segments. Parameter fields have been determined for the relative viscosity of veins and layers, and the kinematic vorticity number of flow. Reworked segment structures can have several shapes such as bone-, bulging, shortened bone-boudins and their asymmetric equivalents such as domino- and shearband-boudin geometry. The model for asymmetric reworked segment structures is applied to such features from the Lower Ugab Meta-turbidites in NW Namibia. The model suggests that these structures form where the neck veins are stronger than the boudinaged layer, with a significant simple shear component of the bulk flow. The quartz filled necks in the Lower Ugab are therefore stronger than the quartz-rich wall rock in greenschist facies where the progressive deformation occurred. Bone-boudins are usually interpreted to form in transpressional flow, but simulations of the rotation of tension gashes show that they can also form in simple shear or slightly transtensional shear flow.

1. Introduction

Boudinage structures are very common in deformed layered rocks in all tectonic contexts and have been an important marker of deformation since the first recognition of pinch-and-swell structures (Ramsay, 1881; Harker, 1889). They are usually defined by the disruption of layers, lenses or foliation planes in response to bulk extension along the enveloping surface (Twiss and Moores, 2007; Ramsay and Huber, 1983). The first use of the term "boudin", however, was to describe cylindrical bodies of deformed sandstone separated by regularly spaced quartz veins, features which have since locally been renamed as double-sided mullions (Lohest et al., 1908; Urai et al., 2001; Kenis et al., 2004, 2005; Sintubin, 2008), while similar structures were elsewhere described as shortened boudins (Passchier, 1991; Passchier and Trouw, 2005). These structures are not thought to have formed by significant extension, but by a two-stage process where a vein network first formed due to enhanced fluid pressure in an environment of low differential stress, generating quartz veins at right angles to layering (Kenis et al., 2002); this was followed by ductile shortening along the layers where a difference in rheology between the sandstone and the veins causes the formation of cuspate structures. Boudins formed by extension parallel to layering and double-sided mullions or shortened boudins can have very similar geometry because all form in response to a periodic gradient in flow parameters along layers.

Many boudin or mullion structures are asymmetric in the sense that they have a monoclinic rather than orthorhombic geometry (Goscombe et al., 2004a). Some of these can be classified as flanking structures (Coelho et al., 2005; Passchier, 2001), fault drag or "hook folds" (Hudleston, 1989; Grasemann et al., 1999). Although most structures have similar geometry on both sides of an affected layer, creating folds of similar axial plane but opposite facing (Fig. 1), some structures in graded bedding develop only on one side of a layer and thus have an even lower symmetry.

Boudins, asymmetric boudins, pinch-and-swell structures, double-sided mullions, shortened boudins, flanking structures and drag folds can all have similar 3D geometry but different inferred mechanisms of formation. We believe that in such cases, the names of structures should reflect their geometry rather than their mechanisms of formation, which is usually hard to reconstruct in the field. For this reason, and since no consensus exists as yet on

* Corresponding author. Laboratory for Mechanics of Materials and Nanostructures, Empa - Materials Science & Technology, 3602 Thun, Switzerland. Tel.: +41 332282959.
E-mail address: xavier.maeder@empa.ch (X. Maeder).

0191-8141/$ – see front matter © 2009 Elsevier Ltd. All rights reserved.
doi:10.1016/j.jsg.2009.05.013

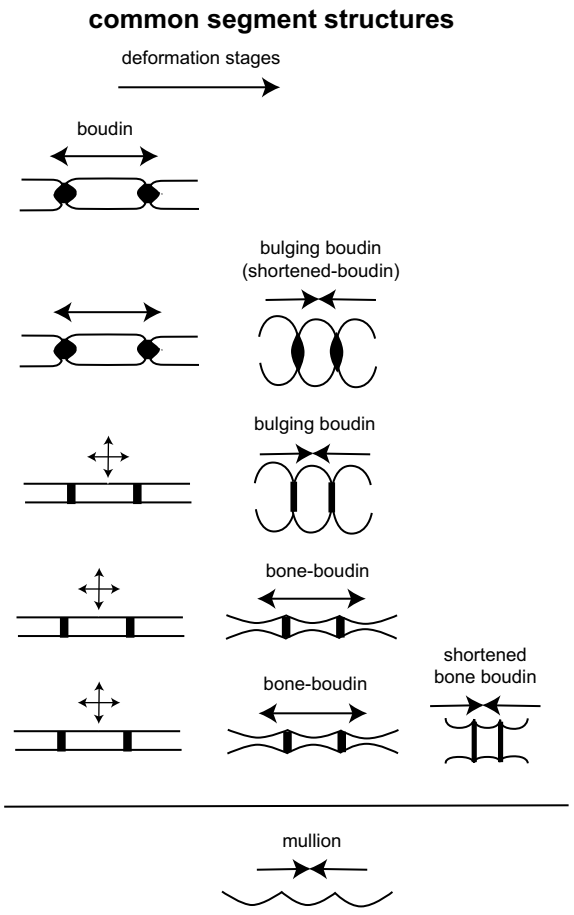

Fig. 1. Terminology of segment structures discussed in this paper.

nomenclature, we will use the general name "segment structures" for all the types of structures treated in this paper. The term "boudin" is specifically used here for deformation structures characterised by veins in thinnest, parts of a planar body of rock, dividing it into barrel-shaped segments; in most cases, boudins will have formed by a process of layer-parallel extension. We use the term "mullions" exclusively for fluted and cusp-like corrugations in rock interfaces where veins are absent in the cusps, and "bulging-boudin" for boudin-like structures with a prominent convex shape and high thickness to length ratio. Such structures can be named "shortened boudins" (Passchier, 1991; Passchier and Trouw, 2005) if they can be shown to have formed by polyphase deformation.

The geometry and asymmetry of segment structures can form in one generation of non-coaxial flow, or by several generations of deformation. Segment structure geometry can therefore be an important indicator of the evolution of local deformation. We modelled development of segment structures with a finite element program to test the influence of the nature of the flow, the original geometry of the structures, and the relative viscosities of the affected layers and of foreign material in the necks on the shape of the final segment structures.

This study on the development of asymmetric segment structures builds onto earlier analogue and numerical modelling work of so-called flanking folds (Grasemann et al., 2003; Wiesmayr and Grasemann, 2005; Kocher and Mancktelow, 2005, 2006; Exner et al., 2004, 2006). Grasemann et al. (2003) and Wiesmayr and Grasemann (2005) used the finite element program BASIL (Barr and Houseman, 1992, 1996) to investigate the development of flanking folds at different matrix flow vorticity and initial orientation of the crosscutting element to the shear zone boundary. The present study provides information about the development of asymmetric flanking folds at the tip of segment structure necks in layers deformed by coaxial and non-coaxial flow.

Comparison of numerical models with natural structures has been used to constrain the influence of flow parameters and rheology (Kocher and Mancktelow, 2005; Kenis et al., 2004, 2005, 2006). Kenis et al. (2004, 2005, 2006) performed a parameter-sensitive analysis on pure shear deformation of segment structures centred on quartz veins to illustrate the effect of original geometry, finite strain, competence contrast between the vein and the rock, and the stress exponent of the constitutive power law on the resulting shape of the structure. The authors used the modelling results as a paleorheological gauge to constrain the relative viscosity of the sandstone in which segment structures developed and of quartz in the veins (Kenis et al., 2005, 2006). We present here a similar parameter-sensitive analysis, conducted on asymmetric segment structures.

In the present study, the finite element program BASIL (Barr and Houseman, 1992, 1996; Houseman et al., 2008) was used to model development of an asymmetric shape by segment structure-neck rotation in non-coaxial flow and the formation of folds. Deformed metaturbidites of the Lower Ugab Domain in NW Namibia provide many examples of segment structures; a detailed structural study on regional deformation and syntectonic veins gives a background to the study of segment structures in the area (Passchier et al., 2002; Maeder, 2007; Maeder et al., 2007).

2. Segment structures in the lower Ugab domain

2.1. Asymmetric and extremely convex segment structures

Segment structures are abundant in metasediments of the Lower Ugab Domain, (Fig. 2; Swart, 1992; Passchier et al., 2002) at the junction of the Kaoko and Damara Mobile Belts in NW Namibia (Miller et al., 1983; Miller and Grote, 1988; Hoffman et al., 1994). The area consists of siliciclastic and carbonate metaturbidites of Neoproterozoic age affected by three phases of late Proterozoic or Cambrian deformation (Passchier et al., 2002). D1 is an event of E–W transpression with a strong component of sinistral shear that formed kilometre-scale N–S to NW–SE trending W-vergent folds with subhorizontal axes (Fig. 2). D2 is a phase of E–W shortening that formed coaxial open folds, mostly in the long flat limb of D1 folds. D1 and D2 occurred at peak regional metamorphic conditions in greenschist facies in the biotite zone (Goscombe et al., 2004b). D3 produced E–W to NE–SW trending minor folds and foliations, associated with a late N–S shortening event. Sets of composite quartz and calcite veins formed in the metasediments during D1, mostly in the pelitic domains. The veins described here are short and lenticular, oblique to D1 folds axes, which developed in pelitic and marble layers (V_A veins in Figs 2 and 3; Maeder et al., 2007; Maeder, 2007). The veins mainly formed in the apparently less competent layers of the siliciclastic formations, which is unexpected for fracturing. Vein-formation the layers was probably assisted by high fluid pressure. The large density of veins and the narrow spacing between veins, as well as the abundant development of vein networks in the marble beds are indications for hydrofracturing. Another possibility is that the sand layers were not fully lithified when the veins formed. The bedding surface close to the tips of the dominant vein type, V_A veins, is deflected into asymmetric flanking folds (Passchier, 2001; Grasemann and Stüwe, 2001; Grasemann et al., 2003) that give the bedding segments a characteristic asymmetric boudin shape that can be found throughout the area (Figs 2 and 3). Boudin-neck veins lie oblique to bedding with variable orientation; veins at the smallest angle to bedding are most deformed and in many cases themselves boudinaged. Veins normal to bedding are undeformed

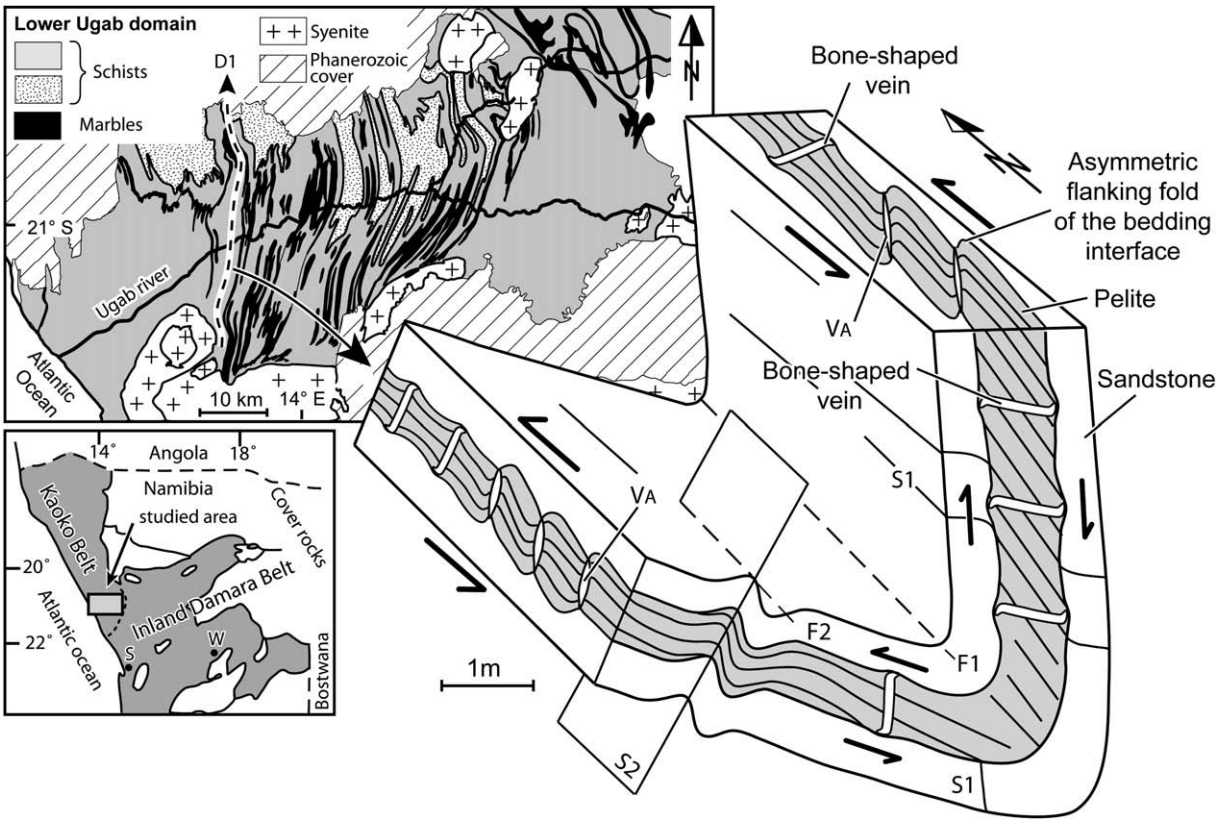

Fig. 2. Geological map of the lower Ugab domain in NW Namibia (modified after Miller and Grote, 1988) with the representation of a W-vergent F1 fold in siliciclastic metasedimentary rocks. V_A developed oblique to the D1 fold axis. V_A veins are affected by sinistral non-coaxial flow which formed flanking folds alongside the veins and an asymmetric shape of the segment structures. There are two generations of bone-boudins, one with roughly east–west trending necks at high angle to D1 fold axis and one with roughly north–south trending necks parallel to D1 fold axis. S–Swakopmund; W–Windhoek.

and lack flanking folds. These observations indicate that the gradient in angle can be interpreted as an effect of various degrees of relative rotation of veins and bedding. The veins would stretch in response to relative rotation with respect to the bedding, causing the boudinage of the veins themselves. Originally symmetric segment structures were therefore deformed into asymmetric shapes by ongoing sinistral non-coaxial flow, mainly during the transpressional D1 deformation. Non-sheared segment structures in low strain areas show that the veins were originally oriented at a high angle to bedding before their rotation in non-coaxial flow. Boudinage of boudin-neck veins themselves, an S3 foliation in the boudins and an extreme convex bedding interface indicate a component of shortening parallel to layering. In the pelites, S3 is steep with an approximately ENE–WSW trend and is in general axial planar to the asymmetric folds" in the layer contact that define the shape of the boudins (Fig. 3(a). The asymmetric geometry of boudins is therefore the combined effect of transpressional sinistral shearing during D1, shortening perpendicular to the layer during D2 and a shortening parallel to the layers during D3 (Fig. 4). In areas with a weak sinistral deformation, bulging boudins occur with a symmetric and extremely convex shape (Goscombe et al., 2004a), similar to "double-sided mullions" described by Urai et al. (2001) and Kenis et al. (2004, 2005), with a symmetric deflection of the bedding between the necks due to layer-parallel compression (Fig. 3(c)).

2.2. Bone-boudins

Bone-boudins as described by Malavielle and Lacassin (1988) appear both in pelite and folded limestone layers of the Lower Ugab Domain, but are more common in the limestone (Figs. 2 and 3(d)). There are two generations of bone-boudins. One is observed in sections parallel to D1 fold axes with necks at a high angle to the fold axes, with an east–west strike. The other generation is observed in sections perpendicular to the D1 fold axes with necks roughly parallel to the fold axes and a roughly north–south strike (Fig. 2). The two generations of bone-boudins formed in both limbs of the D1 folds. In both cases the necks lie at a high angle to the bedding.

Bone-boudins in sections parallel to the D1 fold axes with east–west neck strike have generally a sigmoid shape. The sigmoid shape is created by the bending of the tips of the veins and is generally associated with flanking folds alongside the vein, suggesting that the veins underwent sinistral rotation with respect to bedding. They are therefore associated with V_A veins of roughly similar strike and which underwent the same sinistral rotation. However, the original orientation of the necks of bone-boudins was originally probably oblique to the bedding, since the necks lie roughly perpendicular to the bedding after sinistral rotation. These veins may therefore have formed as tension gashes during the early D1 deformation due to the sinistral shearing component of the bulk flow. Some segment structures with undeformed neck veins may have formed originally at a high angle to the bedding like the V_A veins. The bone-shape may then have resulted from further north–south ductile extension of the layer that contains the veins.

Bone-boudins in sections perpendicular to the fold axes, with roughly north–south strike generally also show a sigmoid shape with development of flanking folds along their side, indicating a reorientation (Fig. 2). The sigmoid shape and the flanking folds indicate two opposite shearing directions in the two limbs. The shear senses are consistent with flexural slip along the flanks of the D1 folds. The veins may have also initially formed as bedding-oblique tension

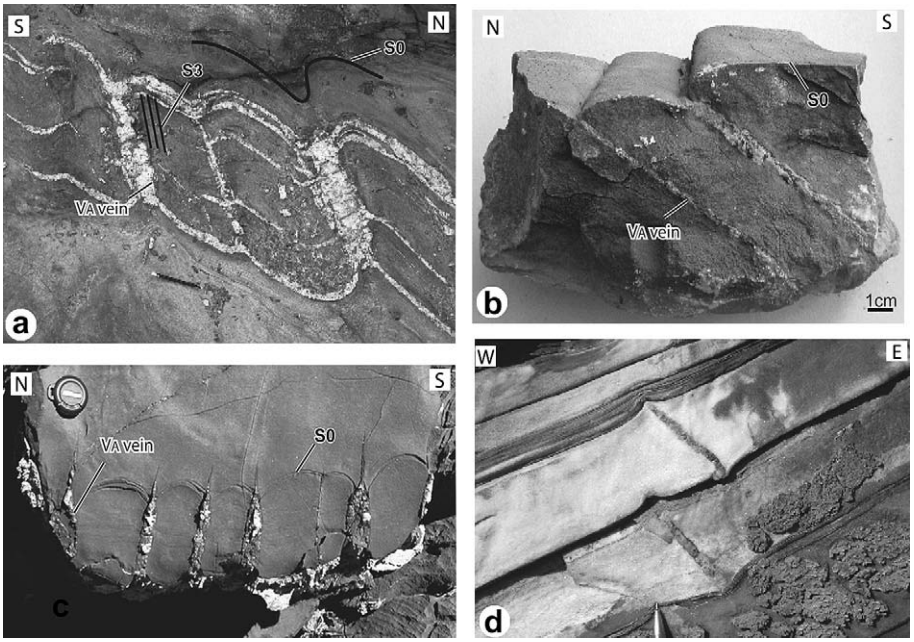

Fig. 3. (a) – (b) Examples of asymmetric segment structures in pelites and marbles in the Lower Ugab region. (c) Example of a bulging boudin with an extreme convex surface between the necks, indicating shortening parallel to the layer (d) Example of a bone-boudin. Locations: (a) −21,07974°/13,81535; (b) −20.83929°/14.13401°; (c) −21.006254°/14.03498°; (d) −21.09104°/13.82326°.

gashes along the flanks at the early stage of flexural slip or as bedding-normal veins due to the extension along the limbs caused by east–west D1–D2 shortening during tightening of D1 folds.

3. Numerical technique

The program "BASIL" of Barr and Houseman (1992, 1996; Houseman et al., 2008) has been used to model rotation of neck veins and the formation of flanking folds along the rotating veins in segment structures. BASIL is a two-dimensional finite element program that can be used to model non-coaxial bulk flow. In the natural examples, the veins and flanking fold structures are mostly cylindrical in three dimensions (Fig. 3(b)) and therefore BASIL is well-suited for the dynamic interpretation.

3.1. Mesh generation and boundary conditions

Three different meshes have been used, all composed of a square divided by three horizontal parallel layers, one internal and two externals (Fig. 5). The internal layer is cut by one or two veins. The viscosity of the internal layer, the two external layers and the veins is variable. The internal layer represents the boudinaged layer in natural examples. It therefore represents the pelitic layer in the siliciclastic formations, while the two external layers model the fine-grained sandstone layers. In the carbonate formations, the internal layer is the boudinaged marble layer and the external layers are the two neighbouring non-boudinaged marble layers. We assumed in the model that the two external layers show the same viscosity. The first and second meshes present respectively one or two veins that cut the internal layer at right angles (Fig. 5(a,b)). The third mesh presents two veins at 135° to the shear zone, which is the orientation of the formation of tension-gash veins, oriented parallel to the shortening instantaneous stretching axis of isochoric plane strain in dextral simple shear flow (Fig. 5(c)). The three meshes include horizontal passive markers named "A, B, C, D, E, F, G, H" (Fig. 5(d)). The markers are parallel to the shear zone boundaries, and consequently taken parallel to the fabric attractor of the flow (Passchier, 1997). "A" is at the centre of the internal layer and "C" is the contact surface between the layers (bedding interface). For reference, the side length of the squares of the mesh is 1.

The grid in the meshes is generated with a self-meshing routine, which creates rectangles subdivided by diagonals in alternating directions for the two first types of mesh and diagonal in one direction for the third type. The model includes a region of 25 by 25 elements for the mesh with a single vein and 30 by 30 elements for the meshes with two veins. The relatively simple geometry of the mesh allows high strain deformation. Finer meshing and a grid composed of triangles with hexagonal symmetry have been tested and do not influence the general shape of the segment structures. Boundary conditions were defined to approximate ideal simple shear and general shear (Grasemann et al., 2003; Wiesmayr and Grasemann, 2005). Steady flow is assumed, so that the incremental strain matrix does not change during the deformation history; during each experiment, the stretching rate factor and the kinematic vorticity number (Wk) remain constant. Wk defines the boundary flow and corresponds to the cosine of the angle a between the irrotational material lines (eigenvectors). Wk = 0 for pure shear and Wk = 1 for simple shear (Means et al., 1980).

4. Parameter-sensitivity analyses

The aim of the numerical approach is to see how conditions of flow, competence contrast between the deformed layers, the external layers and the veins, and the initial geometry of the vein segments before ductile deformation influence their final shape. A parameter sensitivity analysis was performed, and in each experiment only one parameter varies, the others being fixed at a certain value (default value). The following parameters have been investigated:

1. Finite strain
2. Boundary flow conditions (kinematic vorticity number Wk)
3. Competence contrast between layers and veins.
4. Initial aspect ratio of the layer segments
5. Thickness of the veins
6. Stress exponent

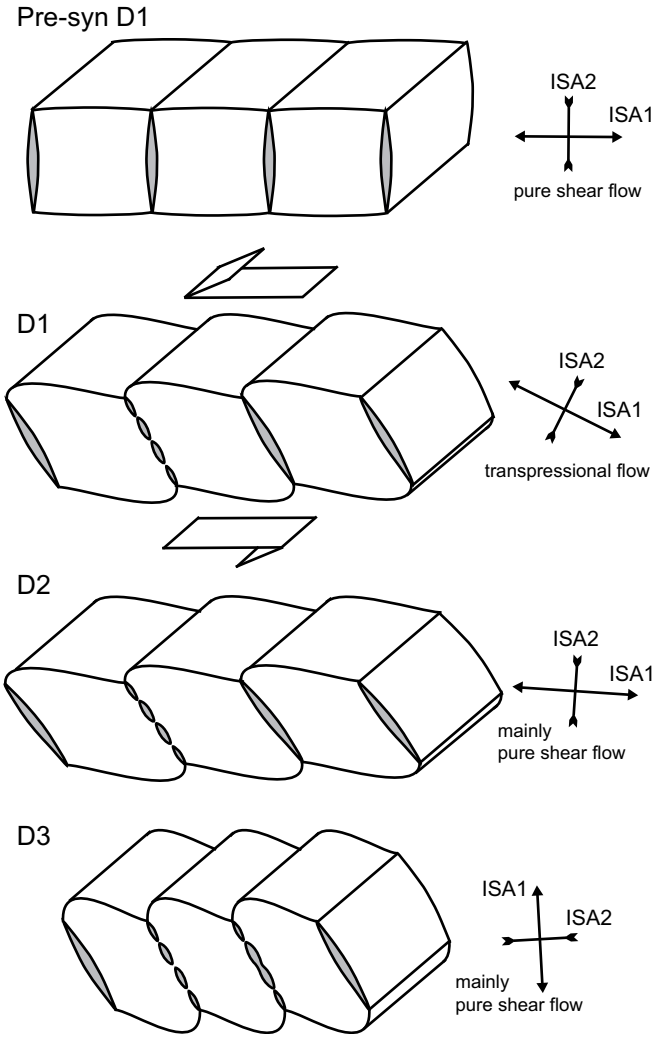

Fig. 4. Polyphase deformation of asymmetric boudins in the Lower Ugab Domain. (a) pre-D1 separation of a layer into segments and deposition of regularly spaced quartz and calcite veins. (b) D1 transpressional phase of deformation caused the rotation of the veins and the formation of the asymmetric flanking folds at the tips of the veins, marked by the bedding interface. (c) D2 deformation caused mainly shortening perpendicular to the layer without much effect on their shape. (d) D3 caused shortening parallel to the layer which led to the development of a pronounced boudin geometry.

Kenis et al. (2005) argue from their simulations that at middle crustal condition, psammite or polyphase quartz-rich rocks seem to be significantly weaker than wet quartz and that rocks seem to behave Newtonian during deformation. In all our field observations in Namibia, vein quartz was apparently stronger than the wall rock during subsequent deformation. Since the neck veins are mainly composed of quartz, they are therefore fixed at a viscosity value ten times stronger than the wall rock during the experiments where we vary the other parameters. By default, the n-exponent is also fixed at 1, and therefore Newtonian deformation is considered. The three layers are fixed by default at the same viscosity for investigating of the influence of the other parameters.

A terminology of flanking fold geometry both in terms of qualitative classification and quantitative description by Bézier curves is given by Coelho et al. (2005) and used in this paper with some modifications. In this terminology, slip defines the displacement of bedding along a vein; roll the degree of rounding of the flanking fold in the bedding adjacent to the vein, and lift the elevation of the bedding with respect to the vein-bedding intersection, measured at some distance from the vein outside the reach of the flanking fold (Coelho et al. (2005). The asymmetric flanking fold marked by the bedding at the tip of the necks of investigated deformed layer segments present no slip and minor lift (Coelho et al., 2005). The asymmetric shape of the structure is marked by an over- or neutral-roll with bulge geometry on one side of the vein and a neutral-roll without bulge on the other side of the vein(Coelho et al., 2005). In order to compare the different shape of flanking folds between different simulation results, we introduce three parameters; the maximum elevation of the flanking folds (ME), the bulge (B) and the angle β between the horizontal shear zone and the tangent of the folded layer interface (Coelho et al., 2005), which is also an expression of the bulge (Fig. 6).

4.1. Effect of the total finite strain in simple shear flow

The effect of the total strain in simple shear flow on the deflection geometry of the interface layer is illustrated in Fig. 7 with the mesh for one neck region. The viscosity of the internal layer is fixed at the same value as the viscosity of the two adjacent layers and the vein is ten times stronger than the wall rock. Simulations of simple shear deformation up to $\gamma = 3$ are shown. An evolution of the geometry of the asymmetric deflection of bedding at the tip of the vein can be observed with an increase of simple shear deformation. The resulting asymmetric shape of the bedding is similar to what we observed in nature (Fig. 3(a,b)). Elevation and bulge of the bedding interface increases and the angle β decreases with an increase in simple shear deformation (Fig. 7). The bulge becomes positive from $\gamma = 2$ in the presented example. The results show therefore that the total strain and the amount of rotation of the vein are important parameters for the shape of polyphase segment structures. Simple shear flow is enough to cause an asymmetric folding of bedding. The asymmetric geometry can also form without a competence contrast between the layers, but with veins stronger than the host medium. Passive markers in the simulation results show the formation of n-type flanking folds along the rotating veins (no displacement of the passive marker along the two sides of the vein; Passchier, 2001) (Fig. 7); this is in agreement with the results of numerical simulations by Grasemann and Stüwe (2001) on the rotation of a strong transecting element in simple shear flow along which n-type flanking folds develop.

4.2. Effect of the kinematic vorticity number

4.2.1. Transtensional regime

The effect of a progressive change of the kinematic vorticity number (Wk) in a transtensional regime on the bedding interface of the mesh with two bedding-normal veins is illustrated in Fig. 8(a). In the experiments Wk is varied by a progressive increase in pure shear component of flow, with shortening parallel to the layers. Wk is 1 for simple shear flow and 0 for strictly pure shear flow (Means et al., 1980). The results show that an increase in pure shear increases the maximum elevation of the deflection between the necks significantly. The bulge and the angle β vary only slightly as a function of an increasing pure shear component. In strictly pure shear flow, we obtained typical "bulging-boudin" geometries with extreme convex layer interfaces between the necks. The structure is similar to the "double-sided mullions" described by Kenis et al. (2004) and Urai et al. (2001) with a symmetric deflection of the bedding between necks. The passive markers inside the internal layer (markers A, B) show the development of n-type flanking folds along the veins from $Wk = 1$ to $Wk = 0.89$. The flanking folds are slightly asymmetric near the bedding surface (see marker B). Increasing pure shear component causes a change in geometry

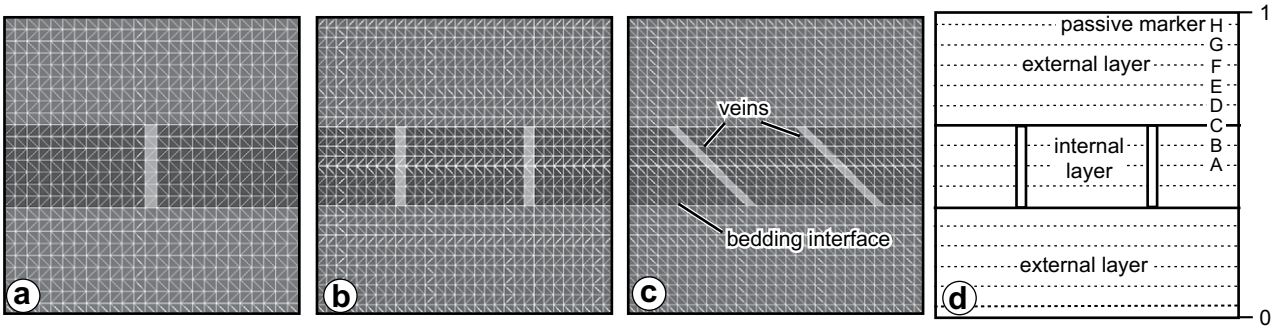

Fig. 5. Three different meshes used in the simulations. All are composed of a square divided by three horizontal layers. Veins cut the internal layer. (a) Mesh with one vein cutting perpendicularly through the internal layer. (b) Mesh with two veins cutting perpendicularly through the internal layer. (c) Mesh with two veins cutting through the internal layer at 135° to the layer. The relative viscosity of the layers and the veins can vary. (d) The meshes have horizontal passive markers (A–H).

towards symmetric folding of the passive marker at both sides of the veins, following the geometry of the layer interface.

The effect of the kinematic vorticity number in transtension with shortening perpendicular to the layers in a mesh with bedding-oblique veins is illustrated in Fig. 8(b). From Wk = 1 to Wk = 0.89, the rotation of the veins lead to bone-boudins as described by Malavielle and Lacassin (1988). Those structures were interpreted to form in a transpressional regime, with the extensional eigenvector parallel to layering (Passchier, 1998; Malavielle and Lacassin, 1988). It is therefore interesting to note that such structures can also appear in a slightly transtensional regime, with the shortening eigenvector parallel to the layer (Passchier, 1998). Occurrence of bone-boudins in the field should therefore not necessarily lead to the interpretation of an extension component parallel to the layer but may also appear in simple shear flow or in a slightly transtensional regime, associated with the rotation of originally bedding-oblique veins. With an increase in shortening parallel to the layer, the geometry of the layer segments tends towards a symmetric deflection of the bedding interface between the necks typical for "bulging-boudin" structures (see marker C). Passive markers A and B in the internal layer show s-type flanking fold geometries with a slight synthetic displacement of the marker along the rotating veins in a transtensional regime (Passchier, 2001) (Fig. 8(b) inset). When the deformation is not strong enough to rotate the veins to a position ≥90° to the shear plane, the passive markers show shearband geometries along the veins, as illustrated by the simulation result of strictly pure shear deformation (Fig. 8(b) inset).

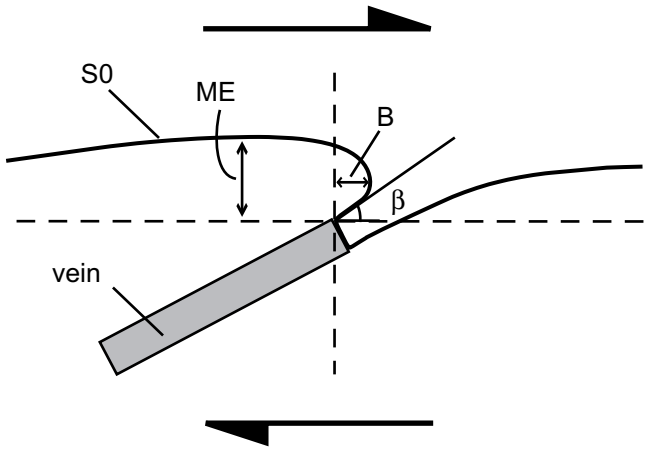

Fig. 6. Drawing of a flanking structure at the tip of a vein. The parameters such as maximum elevation (ME), bulge (B) and β, the angle between the tangent of the flanking folds at the border of the vein and the horizontal, have been used to describe the structure.

4.2.2. Transpressional regime

The effect of a progressive change of the kinematic vorticity number (Wk) in a transpressional regime on the mesh with two bedding-normal veins is illustrated in Fig. 9(a). The pure shear component progressively increases with shortening perpendicular to the layer (extensional stretching eigenvector parallel to the layer; Passchier, 1998). The results show that an increase in shortening perpendicular to the layer slightly decreases the maximum elevation of the flanking folds marked by the bedding interface at the tips of the veins. From Wk = 1 until Wk = 0, the flanking folds always show a slight asymmetry at the tip of the veins. The shortening perpendicular to the bedding in the non-coaxial flow induces passive rotation of the veins. In strictly pure shear flow, the internal layer stretches parallel to the layering between the necks, creating a bone-boudin geometry. The veins remain at their original orientation orthogonal to bedding and act as rigid objects during the compression perpendicular to the layer (veins ten times stronger than the layers). The deformation concentrates in the internal layer that stretches horizontally in the direction of the extensional eigenvector of the flow. The bone-shape geometry therefore is due to the competence contrast between the veins and the layers. This confirms the observations of Kenis et al. (2004, 2006) who show the development of similar bone-shaped structures in their numerical simulations in pure shear flow with extension parallel to the layers with neck veins stronger than the layers.

The effect of the kinematic vorticity number (Wk) in a transpressional regime on the mesh with two bedding-oblique veins is illustrated in Fig. 9(b). An increase in shortening perpendicular to the layers tends to flatten the bedding interface at the tips of the veins. From Wk = 1 to Wk = 0.89 the bedding interface forms a geometry of bone-boudins. From Wk = 0.55 to Wk = 0 the bedding interface remains almost flat. The pure shear component with shortening perpendicular to the layer induces a passive rotation of the veins in a sense opposite to passive material line rotation due to the simple shear flow component. This occurs because of the original oblique orientation of the veins at 45° relative to the layer. From Wk = 0.45, the "counter-rotation" due to the pure shear component of the progressive deformation is more important than the "normal rotation" due to the simple shear component, and the veins are found in a new position with an angle to the bedding that is smaller than 45°. With an increase in shortening perpendicular to the layer the veins become closer to be parallel to the bedding interface. The counter-rotation of the original bedding-oblique veins could lead to an erroneous shear sense interpretation in the field.

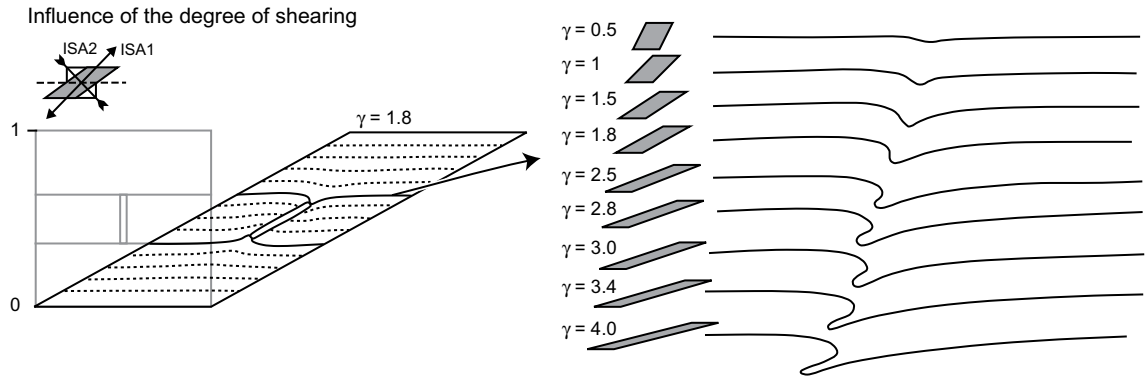

Fig. 7. Diagrams showing the influence of simple shear progressive deformation for the mesh with a single vein. The viscosity of the vein is ten times stronger than the viscosity of the layers. All the layers have the same viscosity.

4.3. *Effect of the competence contrast between the layers*

In these experiments the viscosity of the vein is fixed to a value ten times stronger than the external layers and a simple shear strain of $\gamma = 1.35$ is applied, while the viscosity of the internal layer is varied. Fig. 10(a) illustrates the results of experiments in a mesh with two bedding-normal veins. A weak internal layer implies a stronger rotation of the veins in the simulations because the deformation concentrates in the weakest layer. Both elevation and bulge of the asymmetric flanking folds at the tip of the veins increases with a decrease in the viscosity of the internal layer (Fig. 10(a)). The bulge increases significantly between the two experiments with an internal layer that is 0.5 and 0.25 times weaker than the surrounding layers. Experiments with internal layers stronger than the surrounding layers show very small elevation and develop only weak or no asymmetric shape. The layer interface remains flat in the experiments when the internal layer is 5 times stronger than the surrounding layers.

Experiments of simple shear deformation with $\gamma = 1.35$ and for the meshes with bedding-oblique veins with variable viscosity of the internal layer are illustrated in Fig. 10(b). Only the experiment with an internal layer 4 times weaker than the surrounding layers leads to an asymmetric geometry of the layer interface with positive bulge and elevation. The other simulations show the development of bone-shaped geometries caused by the rotation of the veins in simple shear flow. In the examples where the viscosity of the internal layer is between 2 times weaker than and equal to the viscosity of the surrounding layers, the veins deform slightly into a sigmoid shape caused by their rotation in simple shear flow. Like the simulations with initially bedding-normal veins, the results with an internal layer 5 times stronger than the surrounding layers show flat bedding interfaces with no vein rotation.

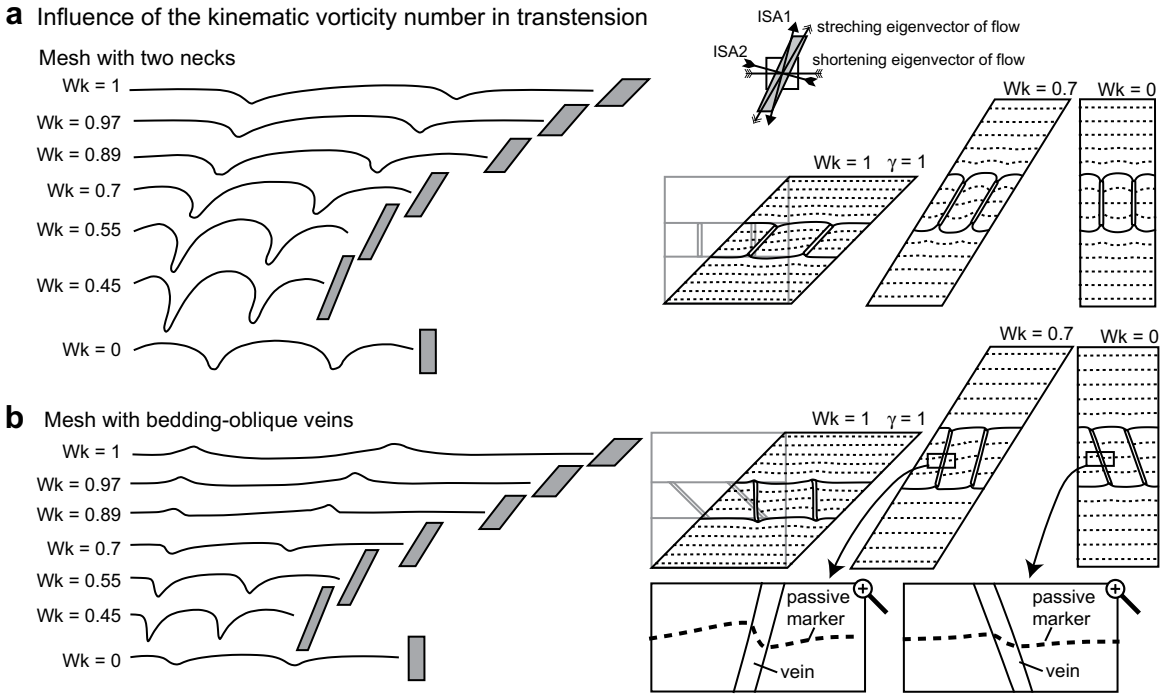

Fig. 8. Diagrams showing the influence of the kinematic vorticity number Wk of the bulk flow in transtensional regime for the mesh with two bedding-normal veins (a) and two bedding-oblique veins (b). We vary the amount of pure shear component for a similar amount of simple shear progressive deformation. The viscosity of the vein is ten times stronger than the viscosity of the layers. All the layers have the same viscosity.

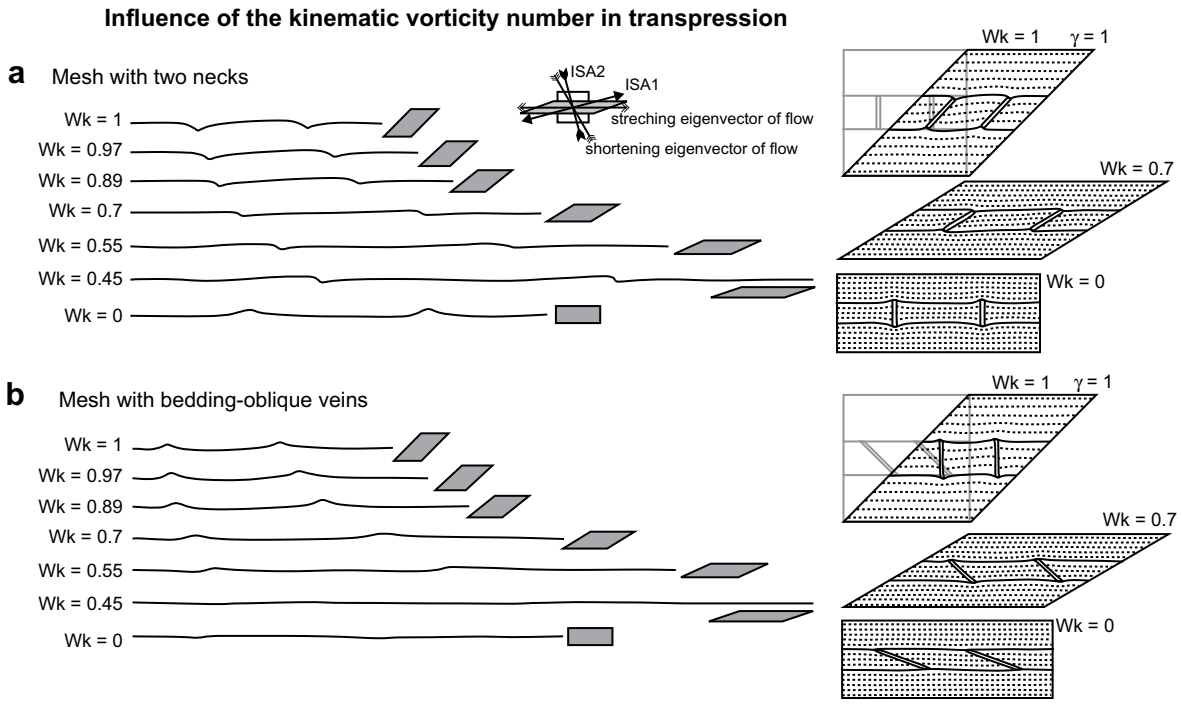

Fig. 9. Diagrams showing the influence of the kinematic vorticity number Wk of the bulk flow in a transpressional regime for the mesh with two necks (a) and two bedding-oblique (b). We vary the amount of the pure shear component for a similar amount of simple shear progressive deformation. The viscosity of the vein is ten times stronger than the viscosity of the layers. All the layers have the same viscosity.

4.4. Effect of the competence of the veins

In these experiments the internal and external layers have a fixed viscosity, the total dextral shear strain is maintained at $\gamma = 1.35$ and the relative viscosity of the vein is varied. Fig. 11(a) illustrates the simulation results for the mesh with two bedding-normal veins. The results show that deflection of bedding increases with an increase in viscosity of the veins. However, the geometry of the deflection remains approximately the same for veins with viscosities 50–1000 times stronger than the layers. The bulge of the asymmetric deflection of the bedding remains approximately the same in all the simulations with veins stronger than the layers, only the elevation increases with an increase in viscosity of the veins. Experiments with veins weaker than the matrix show antithetic slip between the

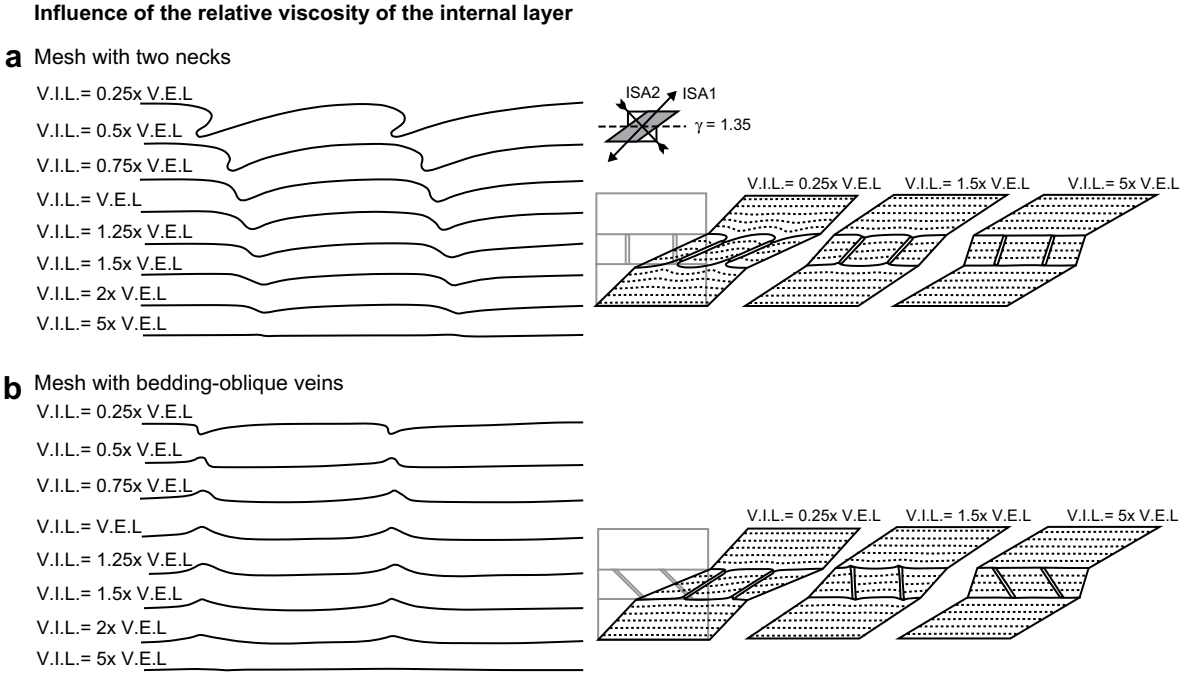

Fig. 10. Diagrams showing the influence of the viscosity of the internal layer for the mesh with two bedding-normal veins (a) and two bedding-oblique veins (b). The meshes have been deformed in simple shear to $\gamma = 1.35$. The viscosity of the vein is ten times stronger than the viscosity of the external layers. The viscosity of the internal layer varies. V.I.L.: viscosity of the internal layer; V.E.L.: viscosity of the external layers.

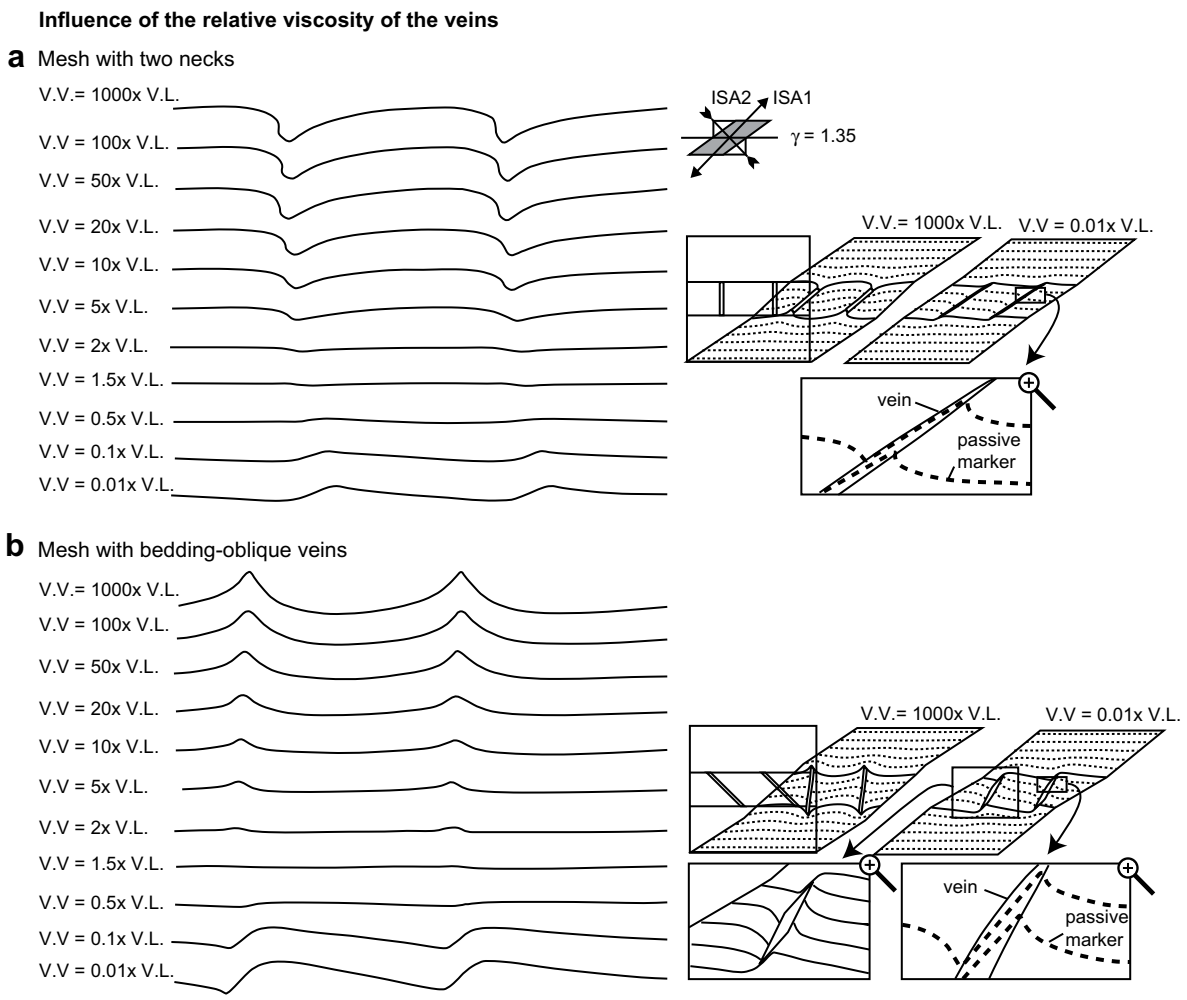

Fig. 11. Diagrams showing the influence of the viscosity of the vein on the mesh with two bedding-normal veins (a) and bedding-oblique veins (b). The meshes have been deformed in simple shear to $\gamma = 1.35$. The viscosity of the three layers is equal. The viscosity of the veins varies. V.V.: viscosity of the veins; V.L.: viscosity of the layers.

layer segments as in domino-boudin structures (Passchier and Druguet, 2002; Goscombe and Passchier, 2003; Gomez-Rivas et al., 2007; Fig. 11(a)). The weak discontinuities allow slip to occur. The passive markers A and B in the internal layer show n-type flanking folds when the veins are stronger than the layers and a-type flanking folds with reverse drag when the veins are weaker than the layers (Fig. 11(a) inset). This is in good agreement with the results of Grasemann et al. (2003) and Wiesmayr and Grasemann (2005), where the authors show the development of a-type flanking folds with reverse drag and extensional offset (Passchier, 2001) alongside a fault during simple shear deformation when the initial orientation of the fault is at 90° with the shear plane.

The effect of relative viscosity of the bedding-oblique veins under simple shear deformation is illustrated in Fig. 11(b). Strong competence contrast between the veins and the layers strengthened the bone-shape geometry of the bedding interface. The bedding interface remains almost flat in the range of veins with viscosities between two times stronger to two times weaker than the layers. It seems that a vein must at least be two times stronger than the wall rock for bone-boudins to form in simple shear flow. The veins deform into a weak sigmoid shape where their viscosity is in the range of 100–10 times stronger than the layers. The simulations with bedding-oblique veins that are weaker than the layers show antithetic slip along the veins, in accordance with the results with bedding-normal veins. In those cases, the bedding-oblique veins deform into a lozenge shape (Fig. 11(b) inset). The passive makers A and B in the internal layers show a-type flanking folds with reverse drag and extensional offset when the tension gashes are weaker than the layers, as in the simulations with the bedding-normal veins (Fig. 11(b) inset). When the veins are stronger than the layers, the passive markers show n-type flanking folds along the rotating veins.

4.5. Effects of other parameters

Aspect ratio of vein segments seems to have little effect on the geometry of deflections, as is illustrated in the experiments of Fig. 12. Only when the veins are very narrow, the bedding interface between the veins develops a smaller deflection, which can be seen in the example with an aspect ratio of 1:4.

Vein thickness seems to have little effect on the shape of flanking folds, although the elevation of asymmetric flanking folds slightly decreases with increasing vein thickness (Fig. 13). The thickness of the veins does not influence the bulge of the flanking folds.

An increase of the stress exponent (Fig. 14) has minor influence on the shape of the deflection of the bedding. The passage from a Newtonian flow to a non-Newtonian flow (from $n = 1$ to $n = 2$) marks the biggest change with a slight increase of the elevation of the asymmetric deflection of the bedding.

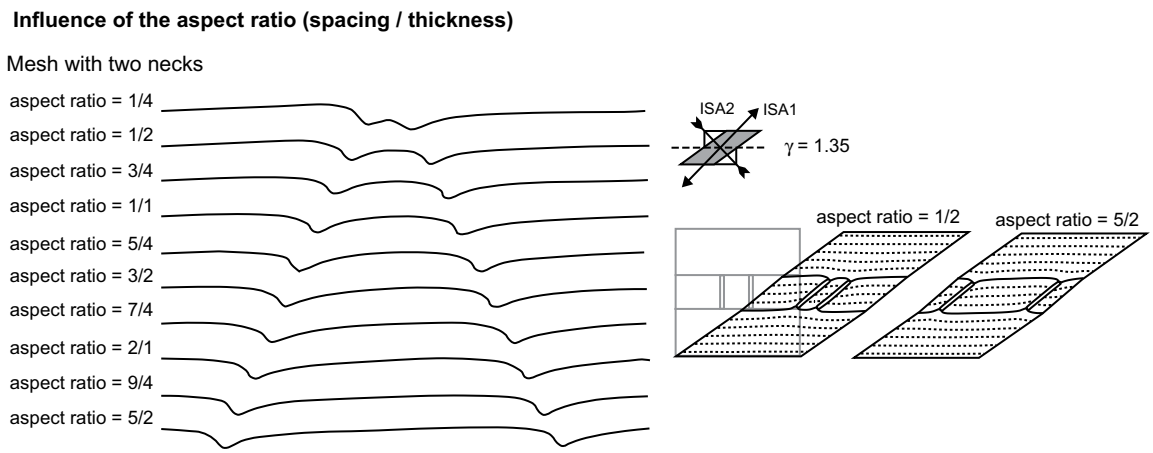

Fig. 12. Diagrams showing the influence of the aspect ratio of layer segments (spacing/thickness). The mesh has been deformed in simple shear to $\gamma = 1.35$. The viscosity of the vein is ten times stronger than the viscosity of the layers. The viscosity of the three layers is equal.

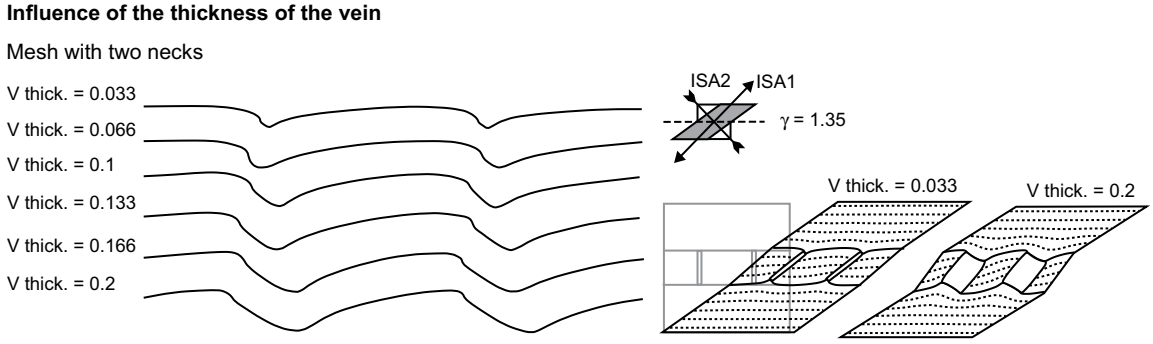

Fig. 13. Diagrams showing the influence of vein thickness. The mesh has been deformed in simple shear to $\gamma = 1.35$. The viscosity of the vein is ten times stronger than the viscosity of the layers. The viscosity of the three layers is equal.

5. Discussion on the parameter sensitivity analyses

The parameter sensitivity analyses show that mainly four parameters determine the shape of segment structures:

1. The total strain
2. The kinematic vorticity number of the flow
3. The competence contrast between the boudinaged layer and the surrounding layers
4. The competence contrast between the veins and the layers.

The aspect ratio of the layer segments, the thickness of the vein and the stress exponent of the power law equation do not significantly influence the geometry of the deflection of the bedding interface. The geometry of the asymmetric flanking folds of the bedding interface adjacent to the neck veins produced in the simulations is very similar to the geometry of natural examples in the Lower Ugab Domain, which confirms our interpretation that the asymmetric shape of segment structures in the studied area results from the rotation of the veins with respect to layering.

Fig. 15 summarises the different shapes of segment structures in relation to the relative viscosity of the veins and the internal layer, and the kinematic vorticity number in transtension and transpression for a certain strain ($\gamma = 2$). Zones can be determined where the segment structures have an asymmetric shape, a domino-, bulging-boudin-, bone- or shortened bone-geometry (Fig. 15).

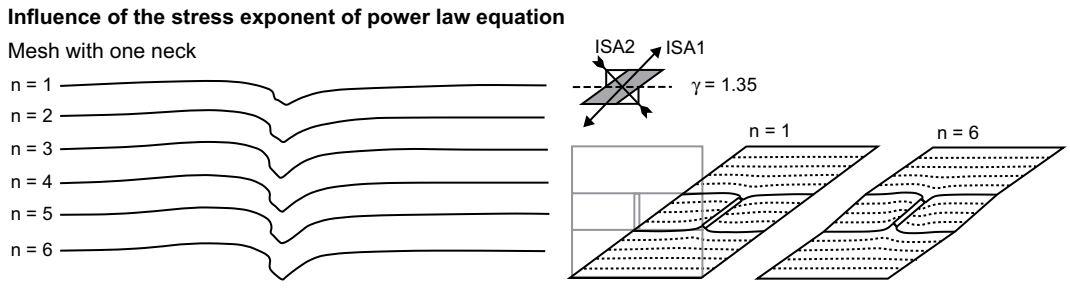

Fig. 14. Diagrams showing the influence of the stress exponent. The mesh has been deformed in simple shear to $\gamma = 1.35$. The viscosity of the vein is ten times stronger than the viscosity of the layers. The viscosity of the three layers is equal.

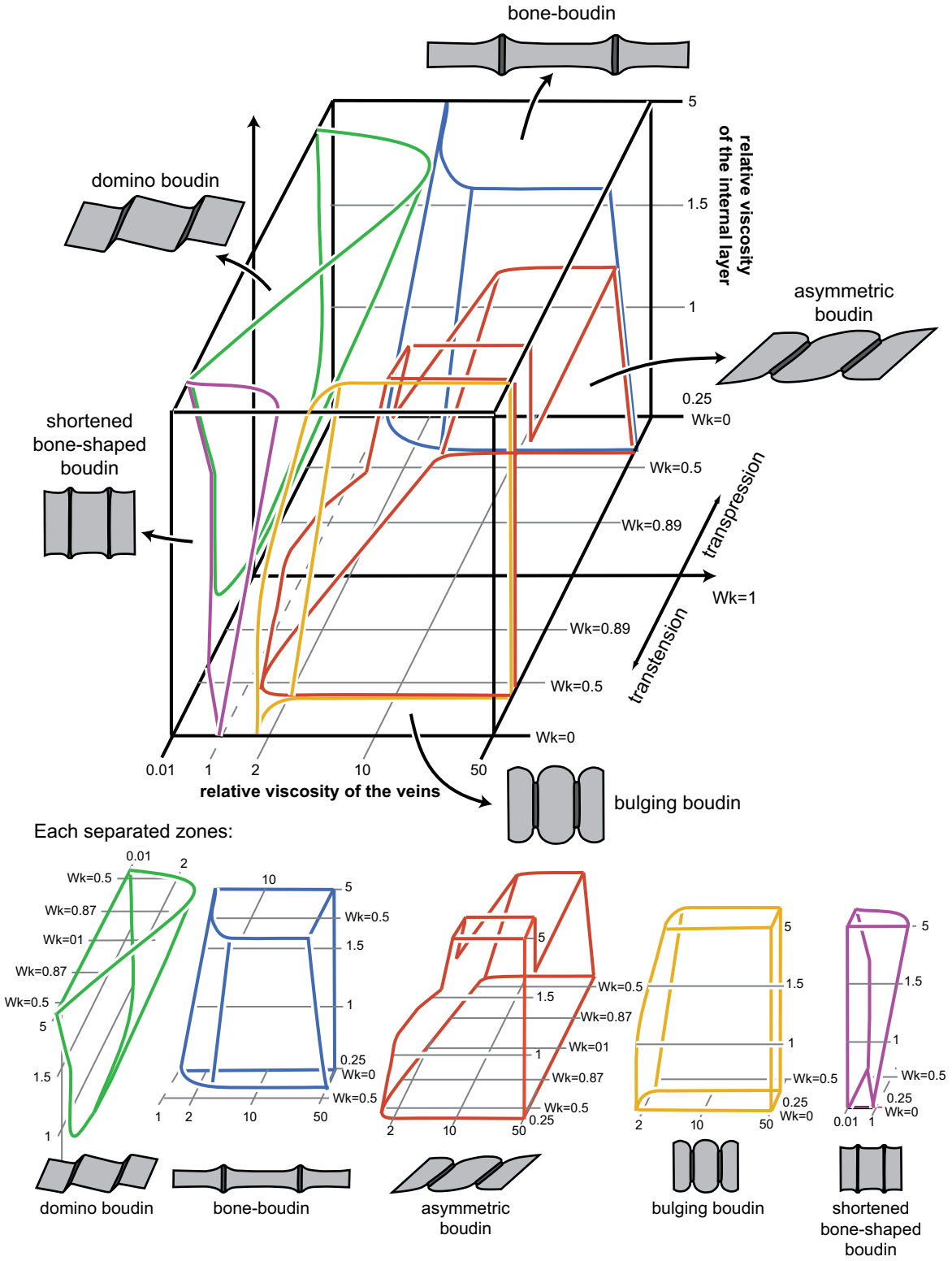

Fig. 15. 3D diagrams showing the repartition of the zones where the segment structures have an asymmetric shape, a bulging-boudin geometry, a domino-boudin geometry, a bone-shape and a shortened bone-shape, according to the three parameters of the relative viscosities of the internal layer and the veins, and the kinematic vorticity number in transpression and transtension.

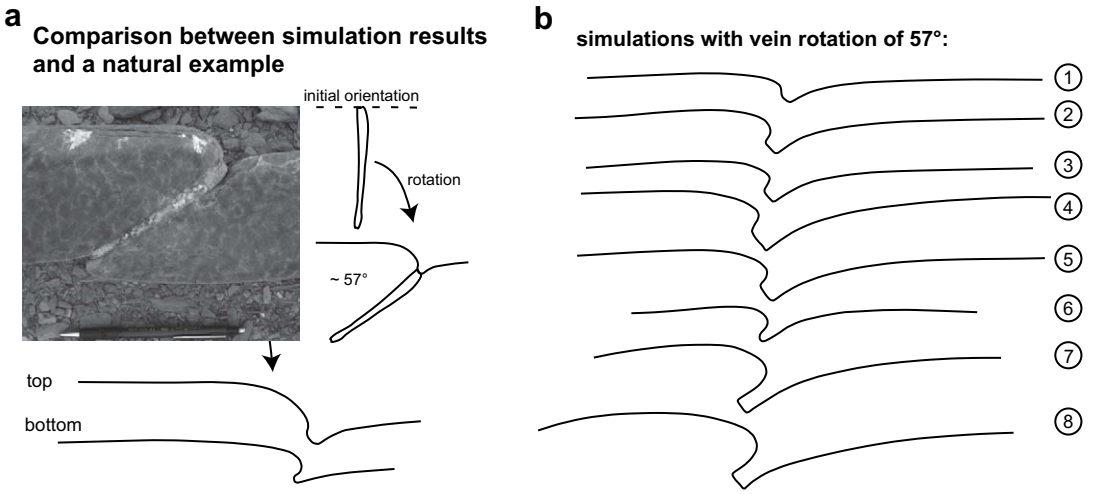

Fig. 16. (a) Example of asymmetric flanking folds at the two tips of a vein in a marble (location: −20.83982°/14.13346°). The vein was probably at a high angle to the bedding before its reorientation oblique to the bedding. This means a rotation of the vein of about 57°. (b) The different parameters which influence the shape of the segment structures are varied in order to find the best fit solution for a comparison with the natural example. Only the bedding interface at the tip of the vein is shown. 1) V.V = 10 × V.E.L., V.I.L. = V.E.L., Wk = 1, γ = 1.7; 2) V.V. = 100 × V.E.L., V.I.L. = V.E.L., Wk = 1, γ = 1.6; 3) V.V. = 50 × V.E.L., V.I.L. = V.E.L., Wk = 1, γ = 1.7; 4) V.V. = 50 × V.E.L, V.I.L. = 0.25 × V.E.L., γ = 1; 5) V.V. = 50 × V.E.L., V.I.L. = 0.5 × V.E.L., Wk = 1, γ = 0.8; 6) V.V. = 10 × V.E.L., V.I.L. = V.E.L., Wk = 0.97; 7) V.V. = 100 × V.E.L, V.I.L. = 0.5 × V.E.L., non-coaxial flow Wk = 0.97; 8) V.V. = 100 × V.E.L, V.I.L. = 0.25 × V.E.L., Wk = 0.97. V.V: viscosity of the vein, V.I.L: viscosity of the internal layer, V.E.L.: viscosity of the external layer.

Asymmetric segment structures occur both in transpression and transtension with a Wk value larger than 0.35–0.25 for veins that are stronger than the internal layers. The asymmetric effect is stronger in a transtensional regime around Wk = 0.5–0.7, where asymmetric segment structures also form for an internal layer 5 times stronger than the external layers, with veins whose relative viscosity exceeds 10 times the viscosity of the external layers. Domino boudins also form in transpression and transtension if Wk is larger than 0.5 and with veins weaker than the internal layer. Domino-boudin geometry is favoured by a high competence contrast between the veins and the internal layer (Fig. 15). Bone-boudins form where the flow is composed of pure shear shortening perpendicular to the layer, or with a small simple shear component (Wk < 0.35). Bone-boudins also form by deformation of bedding-oblique veins with high Wk (0.89–1.0). The veins must be stronger than the internal layer for a bone-shape to form. The bone-shape is favoured by a high viscosity contrast between the veins and the internal layer. Symmetric extremely convex bulging boudins form where the flow is pure shear shortening parallel to the layer, for veins of higher viscosity than the internal layer. Shortened bone-boudins occur where veins have very low relative viscosity and flow is mainly shortening parallel to the layer or has a very small simple shear component. The veins underwent more stretching perpendicular to the layer than the internal layer which produces a bone-shaped geometry of the bedding interface.

6. Comparison between the simulations and the natural structures

Although the rheology of real rocks is more complex than the model in our experiment, a comparison between real cases and the simulations gives interesting results. Fig. 16(a) shows an example from our fieldwork area in Namibia: an asymmetric boudin structure from a marble of the Brandberg West formation. Since non-sheared necks are orthogonal to the layer, the vein is supposed to be originally perpendicular to bedding before rotation. This implies a rotation of °57° with respect to the layering. When the same vein rotation is applied to simulations, it is possible to vary the different parameters to obtain a geometry that is comparable to the natural case. The results are presented in Fig. 16(b). The natural example shows two flanking folds with different maximum elevation at the top and bottom of the beds, but with similar β-angles near 90° and a bulge close to zero (Fig. 16(a)). Solutions 1 or 2 of Fig. 16(b) seem to fit best, with almost neutral bulges. This means that the viscosity of the internal layer (boudinaged layer) could have been about the same as that of the two external layers. It is more difficult, however, to constrain the competence contrast between the veins and the layers, since both simulation examples with veins that are 10 or 100 times stronger than the layers give results that are comparable to the natural example. The use of the geometry of natural examples for a quantitative interpretation, based on the numerical result appears to be difficult. The geometry of the interface between boudin necks varies significantly between different veins of similar orientation in a given layer in the same locality. For example, Fig. 3(b) shows two adjacent veins of similar orientation which most probably underwent the same amount of strain, since they are very narrow and have equal geometry and displacement. The layer interfaces show two different geometries of asymmetric flanking folds at the tip of the veins. The first vein from the left has a clear negative bulge with small elevation and the second a positive bulge with a relatively strong maximum elevation. This means that the shape of the flanking folds can depend on other parameters than the viscosity of the internal–external layers and the veins, the kinematic vorticity of the flow, and the total strain. Local irregularities and undetected elements or clasts in the layers, an effect of sedimentation and diagenetic processes, or slightly different quartz–calcite zonation in the veins can influence the shape of the flanking folds at the tips of the vein. In the simulations, a flat bedding interface of the layer segments is assumed prior to progressive deformation, but formation of torn boudins can lead to barrel-shape boudin geometry with slightly convex bedding interfaces (Goscombe et al., 2004a). An original small-amplitude barrel-shape of undeformed layer segments can influence the shape of the deformed structure (Vanbrabant and Dejonghe, 2006). The exact orientation of the veins with respect to the layering may cause problems. It is possible that some veins opened during the progressive deformation and not during the initial stage of boudinage of the layers.

Even if quantitative estimates of the different parameters are difficult, we can constrain some conditions for the formation of

asymmetric flanking folds at the tip of necks. For an asymmetric flanking fold with positive elevation to develop, the rotating vein must be at least stronger than the internal layer. The internal layers must also be of the same strength or weaker than the external layers. The internal layer can also be slightly stronger than the external layers (in the order of 1.5–2 times) if the shear strain is high and the competence contrast between the vein and the internal layer is high. The results therefore show that the quartz-rich veins are stronger than the pelite and the marble layer in the Lower Ugab Domain. This confirms that wet quartz in the middle crust in greenschist facies conditions where formation of the segment structures occurs, is stronger than the quartz- and mica-rich sandstone wall rock, as shown by the experiments of Kenis et al. (2005).

The application of numerical simulations to develop paleo-rheological gauges for internal and external layers and veins, and gauges for flow conditions may be possible if the model is refined. It is necessary to have a precise idea of the amount of rotation of the vein. The deformation that the vein and the host rock underwent may be estimated by microstuctural observations, which may allow a better constraint on the competency contrast between the vein and the host rock (Kenis et al., 2004, 2005). Statistical work may be relevant since the shape of the flanking folds varies from one vein to the other in the same layer in nature.

7. Conclusions

Finite element numerical simulations of segment structure-neck rotation in coaxial and non-coaxial flow show that asymmetric flanking folds similar to those observed in the Lower Ugab Domain, Namibia form at the tips of the rotating neck veins, which confirms the field observations. For such structures to form, the neck veins must be stronger than the layer. The quartz veins are therefore stronger than the quartz-rich wall rock in the greenschist facies where the progressive deformation occurred, which confirms the conclusions of Kenis et al. (2005) on segment structures in the Ardennes. The effect of the stress exponent of the power law equation on the shape of segment structures, however, is very small. Because the "noise" of original layer shape and variations in rheology of the layers exceeds that of the effect of stress exponent in the examples from Namibia, it is impossible to estimate the stress exponent value for natural deformation conditions in this case. The same may unfortunately apply to many other areas.

The conditions of formation of different types of segment structures is constrained by the relative rheology of the layers and the veins, and the nature of the flow. Simulations show that symmetric and slightly asymmetric bone-boudins are not necessarily the result of significant layer-parallel extension, but can also form by passive rotation of initially bedding-oblique veins in simple shear or only slightly transtensional flow types, provided necks are stronger than the layers.

Acknowledgements

XM and CWP acknowledge a scholarship from the Deutsche Forchungsgemeinschaft (DFG – PA 578/8-1). We gratefully thank the Schürmann Foundation for financial support for fieldwork in Namibia. Lynn Evans and Bernhard Grasemann are acknowledged for their help with the program BASIL. A big "thank you" to Till Sachau for his help with Linux. Journal reviewers K. Kanagawa and P. Bons are thanked for their comments and suggestions.

References

Barr, T.D., Houseman, G.A., 1992. Distribution of deformation around a fault in a non-linear ductile medium. Geophysical Research Letters 19, 1145–1148.
Barr, T.D., Houseman, G.A., 1996. Deformation fields around a fault embedded in a non-linear ductile medium. Geophysical Journal International 125, 473–490.
Coelho, S., Passchier, C., Grasemann, B., 2005. Geometric description of flanking structures. Journal of Structural Geology 27, 597–606.
Exner, U., Grasemann, B., Mancktelow, N., 2006. Multiple Faults in Ductile Simple Shear: Analogue Models of Flanking Structure Systems, vol. 253. Geological Society, London, Special Publications, pp. 381–395.
Exner, U., Mancktelow, N., Grasemann, B., 2004. Progressive development of s-type flanking folds in simple shear. Journal of Structural Geology 26, 2191–2201.
Gomez-Rivas, E., Bons, P.D., Griera, A., Carreras, J., Druguet, E., Evans, L., 2007. Strain and vorticity analysis using small-scale faults and associated drag folds. Journal of Structural Geology 29, 1882–1899.
Goscombe, B.D., Passchier, C.W., 2003. Asymmetric boudins as shear sense indicators – an assessment from field data. Journal of Structural Geology 25, 575–589.
Goscombe, B.D., Passchier, C.W., Hand, M., 2004a. Boudinage classification: end-member boudin types and modified boudin structures. Journal of Structural Geology 26, 739–763.
Goscombe, B.D., Gray, D., Hand, M., 2004b. Variation in metamorphic style along the northern margin of the Damara Orogen, Namibia. Journal of Petrology 45, 1261–1295.
Grasemann, B., Stüwe, K., Vannay, J.-C., 2003. Sense and non-sense of shear in flanking structures. Journal of Structural Geology 25, 19–34.
Grasemann, B., Stüwe, K., 2001. The development of flanking folds during simple shear and their use as kinematic indicators. Journal of Structural Geology 23, 715–724.
Grasemann, B., Fritz, H., Vannay, J.-C., 1999. Quantitative kinematic flow analysis from the Main Central Thrust Zone (NW-Himalaya, India): implication for a decelerating strain path and the extrusion of orogenic wedges. Journal of Structural Geology 21, 837–853.
Harker, A., 1889. On local thickening of dykes and beds by folding. Geological Magazine 6, 69–70.
Hoffman, P.F., Swart, R., Freyer, E.E., Guowei, H., 1994. Damara Orogen of Northwest Namibia. In: Niall, M., McManus, C. (Eds.), Geological Excursion Guide of the International Conference Proterozoic Crustal and Metallogenic Evolution. Geological Society and the Geological Survey of Namibia, p. 55.
Houseman, G.A., Barr, T., Evans, L., 2008. Basil: stress and deformation in a viscous material. In: Bons, P., Koehn, D., Jessell, M. (Eds.), Microdynamics Simulation, Lecture Notes in Earth Sciences, vol. 106. Springer, Berlin-Heidelberg, p. 405.
Hudleston, P.J., 1989. The association of folds and veins in shear zones. Journal of Structural Geology 11, 949–957.
Kenis, I., Sintubin, M., Muchez, Ph., Burke, E.A.J., 2002. The "boudinage" question in the High-Ardenne Slate Belt (Belgium): a combined structural and fluid-inclusion approach. Tectonophysics 348, 93–110.
Kenis, I., Urai, J.L., van der Zee, W., Sintubin, M., 2004. Mullions in the High-Ardenne Slate Belt (Belgium): numerical model and parameter sensitivity analysis. Journal of Structural Geology 26, 1677–1692.
Kenis, I., Urai, J.L., van der Zee, W., Hilgers, C., Sintubin, M., 2005. Rheology of fine-grained siliciclastic rocks in the middle crust-evidence from structural and numerical analysis. Earth and Planetary Science Letters 233, 351–360.
Kenis, I., Urai, J.L., Sintubin, M., 2006. The development of bone-shaped structures in initially segmented layers during layer-parallel extension: numerical modeling and parameter sensitivity analysis. Journal of Structural Geology 28, 1183–1192.
Kocher, T., Mancktelow, N.S., 2005. Dynamic reverse modelling of flanking structures: a source of quantitative kinematic information. Development in anisotropic viscous rocks. Journal of Structural Geology 27, 1346–1354.
Kocher, T., Mancktelow, N.S., 2006. Flanking structure development in anisotropic viscous rocks. Journal of Structural Geology 28, 1139–1145.
Lohest, M., Stainier, X., Fourmarier, P., 1908. Compte rendu de la session extraordinaire de la Société Géologique de Belgique, tenue à Eupen et à Bastogne les 29, 30 et 31 Août et le 1, 2 et 3 Septembre 1908. Annales de la Société Géologique de Belgique 35, 351–434.
Maeder, X., 2007. The Interaction of Veins and Foliations in Metaturbidites of the Lower Ugab Domain, NW Namibia. PhD thesis, Johannes Gutenberg University of Mainz, p. 160.
Maeder, X., Passchier, C.W., Trouw, R.A.J., 2007. Flame foliation: evidence for a schistosity formed normal to the extension direction. Journal of Structural Geology 29, 378–384.
Malavielle, J., Lacassin, R., 1988. "Bone-shaped" boudins in progressive shearing. Journal of Structural Geology 10, 335–345.
Means, W.D., Hobbs, B.E., Lister, G.S., Williams, P.F., 1980. Vorticity and non-coaxiality in progressive deformations. Journal of Structural Geology 2, 371–378.
Miller, R.McG., Freyer, E.E., Hälbich, I.W., 1983. A turbidite succession equivalent to the entire Swakop Group. In: Miller, R.McG. (Ed.), Evolution of the Damara Orogen. Special Publication of the Geological Society of South Africa, vol. 11, pp. 65–71.
Miller, R.McG., Grote, W., 1988. Geological Map of the Damara Orogen of South West Africa/Namibia. Geological Survey of Namibia. scale1:500.000.

Passchier, C.W., 1991. Deformation in the proterozoic revenue granite pluton, Mt Isa Inlier, Australia. Geologie en Mijnbouw 70, 275–285.
Passchier, C.W., 1998. Monoclinic model shear zones. Journal of Structural Geology 20, 1121–1137.
Passchier, C.W., 1997. The fabric attractor. Journal of Structural Geology 19, 113–127.
Passchier, C.W., 2001. Flanking structures. Journal of Structural Geology 23, 951–962.
Passchier, C.W., Druguet, E., 2002. Numerical modelling of asymmetric boudinage. Journal of Structural Geology 24, 1789–1803.
Passchier, C.W., Trouw, R.A.J., Ribeiro, A., Paciullo, F.V.P., 2002. Tectonic evolution of the southern Kaoko belt, Namibia. Journal of African Earth Sciences 35, 61–75.
Passchier, C.W., Trouw, R.A.J., 2005. Microtectonics, second ed. Springer Verlag, Berlin, p. 366.
Ramsay, A.C., 1881. The Geology of North Wales, vol. 3. Memoirs of the Geological Survey of Great Britain.
Ramsay, J.G., Huber, M.I., 1983. Modern Structural Geology. In: Strain Analyses, vol. 1. Academic Press, San Diego, p. 307.
Sintubin, M., 2008. Photograph of the month. Journal of Structural Geology 10, 1315–1316.
Swart, R., 1992. The Sedimentology of the Zerrissene Turbidite System, Damara Orogen, Namibia, vol. 13. Memoir of the Geological Survey of Namibia, p. 54.
Twiss, R.J., Moores, E.M., 2007. Structural Geology, second ed. Freeman, New York. p. 736.
Urai, J.L., Spaeth, G., van der Zee, W., Hilgers, C., 2001. Evolution of mullion (formerly boudin) structures in the Variscan of the Ardennes and Eifel. Journal of the Virtual Explorer 3, 1–15. url: http://virtualexplorer.com.au/2001/Volume3review/Urai2/index.html.
Vanbrabant, Y., Dejonghe, L., 2006. Structural Analysis of Narrow Reworked Boudin and Influence of Sedimentary Successions during a Two-stage Deformation Sequence (Ardenne-Eifel Region, Belgium-Germany), vol. 53. Memoirs of the Geological Survey of Belgium, p. 43.
Wiesmayr, G., Grasemann, B., 2005. Sense and non-sense of shear in flanking structures with layer-parallel shortening: implications for fault-related folds. Journal of Structural Geology 27, 249–264.